Hindawi
Advances in Materials Science and Engineering
Volume 2019, Article ID 3680253, 8 pages
https://doi.org/10.1155/2019/3680253

Research Article

Hydrogen Effect on Cumulation of Failure, Mechanical Properties, and Fracture Toughness of Ni-Cr Alloys

Alexander Balitskii [1,2] **and Ljubomyr Ivaskevich** [1]

[1] *Karpenko Physico-Mechanical Institute National Academy of Sciences of Ukraine, 5 Naukova str., Lviv, Ukraine*
[2] *West Pomeranian University of Technology in Szczecin, 19 Piastow Av., 70-310 Szczecin, Poland*

Correspondence should be addressed to Alexander Balitskii; balitski@ipm.lviv.ua

Received 11 July 2019; Revised 11 September 2019; Accepted 12 September 2019; Published 9 October 2019

Academic Editor: Akbar Heidarzadeh

Influence of hydrogen pressure and internal hydrogen contents on short-term strength, plasticity, and plane-stress fracture toughness of 05Cr19Ni55 alloys at pressure up to 30 MPa was investigated. It was established that the crack resistance parameters K_c of alloys decrease with displacement rates decreasing similar to elongation (δ) and reduction of area (ψ) of smooth specimens. The maximum hydrogen influence is achieved at strain rate speeds less than 0.1 mm/min and hydrogen pressures above 15 MPa when δ and K_c of prehydrogenated samples are reduced by 3 times. The plane-strain conditions required for the evaluation of K_{Ic} were fulfilled on compact tension 05Cr19Ni55 alloy specimens with thickness above 20 mm under hydrogen pressure 30 MPa and preliminary dissolved hydrogen concentration above 20 wppm. Regardless of the test conditions, the value of the characteristics of plasticity (δ, ψ) and fracture toughness (K_c) of alloy (TO1) specimens oriented in the transverse direction (orientation TV) is significantly lower than that of specimens oriented in the longitudinal direction (LT). Alloy cleaning by vacuum arc remelting and optimization of heat treatment regime increase their hydrogen resistance.

1. Introduction

Heat-resistant nickel alloys are widely used in energy and aerospace engineering in contact with high-pressure hydrogen-containing gas mixtures [1–5]. Therefore, one of the most important requirements for such alloys is their resistance to hydrogen degradation. However, it is known that precipitation-hardening alloys are sensitive to hydrogen embrittlement [1–5]. So, for correct estimation of their workability in hydrogen environment, it is important to determine the effect of the structure and parameters of the load on the mechanical properties.

In order to ensure the safety and reliability of materials for a steam and gas turbine, structural integrity and lifetime prediction are of great importance. Working structures and their elements (blades and discs) are subjected to the influence of various loads and hydrogen-containing gas. In order to ensure an adequate level of safety and optimal durability of such structural elements, experimental tests in gaseous hydrogen are required to determine the effect of various factors. By the fracture mechanics approaches, evaluation of static load durability of structures and critical crack (defect) size in technological or operational circumstances have been calculated as the values of critical stress intensity factor K_{Ic} (K_c) [1, 3–6]. Use of this option to evaluate workability details in gaseous hydrogen is limited to a number of factors caused by the methodological aspects of the determination in laboratory conditions and characteristics of initiation and growth of cracks in the presence of hydrogen [3–9]. The materials employed in hydrogen energy should have little sensitivity to cracks and cuts that have a high ability to relax tension in the areas of highest concentration (high plasticity), which does not archive the plane-strain state for research specimens and determines KIc by standard methods in air [5–8]. Therefore, most studies of the impact of hydrogen on mechanical behavior of structural steels and alloys were carried out with tests on short-term static tensile and low-cycle durability [1–3, 10, 11]. The

influence of load conditions (speed for static tension, frequency and amplitude by low-cycle fatigue, temperature, pressure, and dissolved hydrogen content in advance) on strength, ductility, and durability of materials of different structural classes was established [1–4, 11]. However, literature data on regularities of influence of hydrogen on the static crack resistance are limited and controversial [1–5]. The issue of the effect of sample orientation on the sensitivity of materials to the action of hydrogen remains poorly understood. The influence of texture components on hydrogen-induced cracking of pipeline steel has been studied in [12, 13], and similar data on heat-resistant materials are limited and ambiguous [14, 15].

In what follows, we study the influence of high-pressure gaseous hydrogen on short-term strength, plasticity, and static crack resistance of a nickel-based alloy 05Cr19Ni55 with different modes of heat treatment and chemical composition variations.

2. Materials and Experimental Procedure

The alloy 05Cr19Ni55 from which parts used in energy, petrochemical engineering, and aerospace engineering products [16, 17] are manufactured for use in the hydrogen environment has been investigated. Chemical composition of investigated alloys is shown in Table 1. Alloying with niobium, vanadium, titanium, aluminum, and boron leads to the formation of carbides $(Ni, Fe, Cr)_{23}C_6$, borides Me_3B_2, and intermetallics $Ni_3(Al, Mo, Nb)$ in the amounts up to 10%, which substantially increases their high-temperature strength and significantly influences the sensitivity to the action of hydrogen [1–3, 9, 11]. Presented in Table 2 and in Figures 1 and 2 are the results obtained in the first version of the chemical composition (CC).

The orientation of specimens, method of melting, heat treatment regimes, grain sizes, thickness of the specimens for fracture toughness testing, the mechanical properties of alloy in the air and in hydrogen under the pressure of 30 MPa after preliminary hydrogenation (623 K, 30 MPa H_2, 10 h), and coefficients of influence of hydrogen on reduction of area and K_{Ic} are shown in Table 2.

Static tensile tests were carried out on standard fivefold cylindrical specimens with a diameter of working part 5 mm using the strain-rate range $V = 0.01$–100 mm/min. Stress intensity factor under static loading K_c was computed either for the maximum force F_C in the "F-V" linear diagram or for the force F_Q determined by using 5% secant for nonlinear diagrams. Rectangular compact specimens were tested for eccentric tension under the pressures up to 30 MPa at a strain rate of 0.01–100 mm/min. The values of K_c are calculated from the Srawley–Gross formula [18]. Plastic properties of the alloy in the air are so high (see Table 2) that plane-strain conditions on samples with a thickness of 20–25 mm are not implemented. Therefore, plane-stress fracture toughness was determined by the method of J-integral [19]. Despite some reservations, this method is often used to evaluate static fracture toughness of plastic materials and for small thicknesses of parts of structures [1, 6, 7]. For tests, we have used the 50x48x20 mm specimens with previously groved at 293 K fatigue cracks.

Specimens were hydrogenated in a working chamber at 623 K and hydrogen pressure 30 MPa during 1–10 h. The maximum hydrogen content in the specimens varied from 21 wppm to 27 wppm depending on the structural state of the alloy (see Table 2). Hydrogen concentration (C_H) was determined with a LECO TCH 600 instrument [20] with precise 0.1 wppm (3 specimens for point). To determine the indicated mechanical characteristics in hydrogen, the working chambers were preliminarily evacuated, blown-out with hydrogen, again evacuated, and filled up with hydrogen to a given pressure. All tests were performed at room temperature.

3. Results and Discussion

3.1. Influence of Loading Rate on the Cumulation of Failure and Properties in Hydrogen. The behavior of the rate dependences of hydrogen degradation is determined by the kinetics of penetration of hydrogen into the material and changes in the mechanisms of deformation. As the rate of short-term tension decreases, the influence of hydrogen first increases, and then the properties become stable (see Figure 3). Under a constant hydrogen pressure and content, the rate interval and the degree of maximum embrittlement are determined by the chemical composition and the structural state of the material. Substantial reductions in ductility characteristics of the alloy with CC I (see Table 1) after HT III (see Table 2) were found in the range of rates 0.1–10 mm/min and with CC II after HT II in the range 0.1–1 mm/min (see Figure 3, curves 1, 4 and 3, 6).

The maximum embrittlement of hydrogenated material in hydrogen under a pressure of 30 MPa is realized at a rate less than 0.1 mm/min ($0.67 \cdot 10^{-4} \cdot s^{-1}$), which is three orders of magnitude smaller than the regulated rate of determination of the hydrogen resistance of steels with a body-centered cubic structure equal to 10 mm/min [4–7, 11, 12]. This ratio of the rates correlates with the ratio of the diffusion coefficients of hydrogen in alloys with face-centered cubic and body-centered cubic lattices given in [1, 4–7, 11, 21, 22], which testifies to the penetration of hydrogen into the metal in the process of static tension.

Similarly, the level of K_c decreases with decreasing dK/dt to the minimum value, defined of material structural condition (see Figure 1). The widest rate range and greatest sensitivity to the action of hydrogen typical for longitudinal samples after open melting HT1 with a coarse-grained structure (see Figure 1, curve 1). Maximum embrittlement of these specimens and specimens with grain size 36 microns are achieved by loading rate 0.18 MPa·m$^{1/2}$/s (see Figure 1, curves 1 and 8), a grain size of 21 microns, and the largest fracture toughness in the air −0.054 MPa·m$^{1/2}$/s (see Figure 1). At the same time, if in air with increasing thickness of the sample, parameter K_c slightly increases, then in hydrogen, it decreases (see Table 2, positions 5, 6, 7, and 8); i.e., the embrittlement effect of hydrogen on the fracture toughness of the alloy increases.

Table 1: Chemical composition of 05Cr19Ni55 alloy (mass %).

CC	C	Fe	Cr	Mo	Nb	Al	N	∑Cr, Mo, Nb, Fe	∑ N + C	$(Cr, Ni, Fe)_{23}(C, N)_6$
I	0.05	12.0	19.0	8.87	1.73	1.49	0.07	41.60	0.12	3.1
II	0.04	11.0	17.5	8.97	1.84	1.54	0.03	39.38	0.07	2.0

Table 2: Characteristics of the 05Cr19Ni55 alloy modifications at 293 K and displacement rate 0.1 mm/min.

No. of order	Orientation	Heat treatment	d (μm)	t (mm)	K_{1c} (J_c) (MPa·m$^{1/2}$)	C_H (wppm)	σ_u / σ_{ys} MPa	δ / ψ %	K_c (MPa·m$^{1/2}$)	β_ψ / βK_c
1	TV	OM. Quenching (Q): 1323 K, 1 h Aging (A): 1023 K, 15 h, +923 K, 10 h (HT I)	85	20	86	25	920/930	570/570	10/2.5	12/4.5	69/28	0.38/0.32
2	LT	OM, HT I	85	20	107	25	1020/970	590/600	14/4.5	18/8	88/38.5	0.44/0.36
3	LT	VAR, HT I	85	20	128	22	1050/1010	620/610	20/6	32/15	98/51	0.47/0.40
4	LT	OM. Q: 1253 K, 1 h. A: 1023 K, 15H, +923, 10 h (HT II)	21	20	119	27	1040/990	610/610	17/5	20/9	94/45	0.45/0.38
5	LT	VAR, HT II	21	20	162	24	1080/970	650/660	35/6	38/19	116/68	0.50/0.42
6	LT	VAR, HT II	21	25	162	24	1080/970	650/660	35/6	38/19	126/64	0.50/0.40
7	LT	VAR, after HT II simulation of soldering 1283 K, 15 min, A: 973 K, 10 h (HT III)	36	10	138	21	1180/960	710/690	30/5	34/16	103/62	0.47/0.45
8	LT	VAR, HT III	36	20	138	21	1180/960	710/690	30/5	34/15	108/52	0.44/0.38
9	LT	VAR, after HT II simulation of soldering 1473 K, 15 min + 1273 K, 1 h (HT IV)	130	20	—	23	750/700	380/390	41/16	31/18	—	0.58/—

TV: transverse orientation; LT: longitudinal orientation; OM: open melting; VAR: vacuum arc remelting; d: grain size; t: thickness of the specimen. $\beta_\psi = \psi_{hydr}/\psi_{air}$; $\beta_{KC} = K_{c\ hydr.}/K_{Ic(Jc)}$ air.

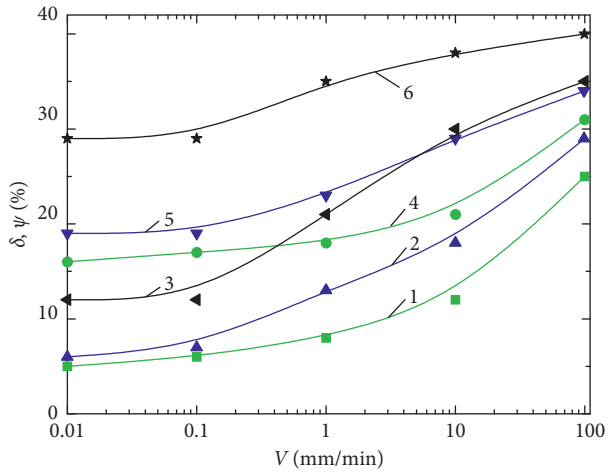

Figure 1: The effect of rising K rate dK/dt on fracture toughness K_c in hydrogen under pressure 30 MPa of hydrogenated specimens of 20 mm thickness. The numbers near to curves correspond to ordinal numbers in Table 2.

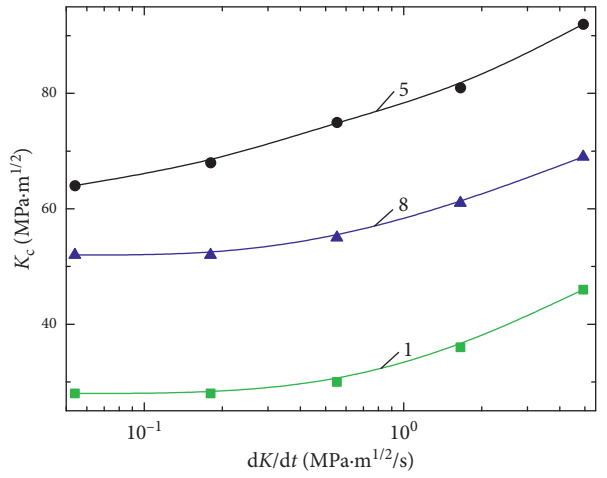

Figure 2: Dependences of fracture toughness K_c of prehydrogenated (623 K, 30 MPa H_2, 10 h) specimens of 20 mm thickness on the hydrogen pressure P at a strain rate of 0.1 mm/min. The numbers near curves correspond to ordinal numbers in Table 2.

3.2. Influence of Hydrogen Pressure on Fracture Toughness. The dependences of the fracture toughness of prehydrogenated specimens on the hydrogen pressure consist of two regions. In the first region (low pressures), the pressure abruptly drops, and in the second, the negative action of hydrogen becomes stable (see Figure 2). This means that there exists a pressure under which degradation of the material with hydrogen reaches its maximum. In our case, this effect is found for pressures more than 15 MPa. Note that the properties of nonhydrogenated specimens of the

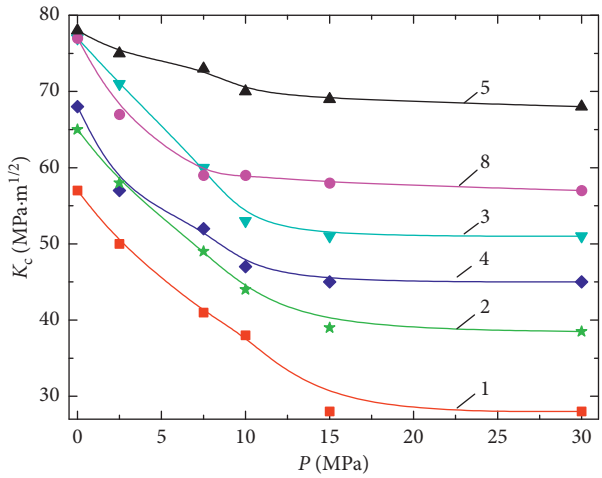

FIGURE 3: Dependences of plasticity characteristics δ (1–3) and ψ (4–6) of prehydrogenated (623 K, 30 MPa H_2, 10 h) specimens in hydrogen under pressure 30 MPa on the strain rate: 1, 4: CC (I) VAR, HT III; 2, 5: CC (I) VAR, HT II; 3, 6: CC II, VAR, HT II.

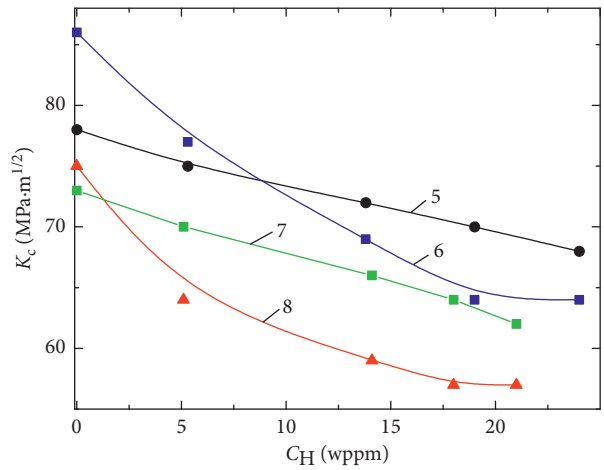

FIGURE 4: Dependences of fracture toughness K_c at hydrogen pressure of 30 MPa of specimens of 10 (7), 20 (5, 8) and 25 (6) mm thickness on the hydrogen content C_H at a strain rate of 0.1 mm/min. The numbers near curves correspond to ordinal numbers in Table 2.

alloy 05Cr19Ni55 do not reach the minimum values in the pressure range 0–35 MPa [11].

In hydrogen under the pressure 30 MPa, K_c of the alloy (CC I after HT II and HT III) of the thickness 20 mm decreases to 68 MPa·m$^{1/2}$ and 57 MPa·m$^{1/2}$ at the hydrogen concentration of 19 and 18 wppm, respectively, and does not change with further hydrogenation (see Figure 4, curves 5 and 8). Under these conditions, the diagrams "load–displacement" are linear with a sharp maximum of the load and fracture surface of specimens covered cleavage facet, typical for brittle fracture. K_c value reaches the critical value K_{1c} that satisfies the condition l, $b \geq 2,5\ (K_c^H/\sigma_{ys}^H)^2$, where l is the crack length and b is the specimen thickness [18, 19]. Thus, hydrogen initiates the destruction of the mechanism of normal separation across the whole crack front, causing formation of the plane-strain state in the specimen. Conditions of the plane-strain state on all modifications of the alloy are performed by the specimen thickness 20 mm with the exception of positions 5 and 7 in Table 2. K_{IcH} alloy with CC I after VAR, HT II (position 5) is equal to 64 MPa·m$^{1/2}$ and achieved on specimens of thickness 25 mm (see Figure 4, curve 6). For a specimen thickness of 10 mm, plane-strain conditions for the alloy (CC I after HT III) did not perform even after the hydrogenation to the $C_H = 21$ wppm (see Figure 4, curve 7). Thus, the maximum effect of hydrogen on fracture toughness of specimens with lower thickness is achieved by more intensive modes of action (hydrogen pressure or content) or slower loading rates (see Figure 1), when conditions are provided to allow sufficient hydrogen to enter the crack tip. At the same time, if in air with increasing thickness of the sample, parameter K_c slightly increases, then in hydrogen, it decreases (see Table 2, positions 5, 6 and 7, 8); i.e., the embrittlement effect of hydrogen on the fracture toughness of the alloy increases.

3.3. Influence of Metallurgical Factors on the Alloy Properties. Strength, plasticity, and fracture toughness of the alloy 05Cr19Ni55, melted in vacuum and open electric furnaces, were compared. For the same heat treatment, the alloy after vacuum arc remelting has much higher plasticity than after open melting (position 2, 3 and 4, and 5 in Table 2). Significantly higher are all crack resistance parameters: $K_{1c}(J_c)$ and K_c on air and K_{1c} prehydrogenated specimens in hydrogen (see Figure 5). The resulting open smelting fine-grained structure under the same conditions absorbs the largest number of hydrogen (position 4 in Table 2). To establish the reasons for increasing the properties of the vacuum alloy was determined gases content (by vacuum melting) and impurities (spectral method). Also conducted chemical and X-ray analysis of phases and studied the structure. It was found that open and vacuum melting alloy containing an identical amount of nitrogen have the same lattice parameters of γ- and γ'-phases.

Chemical composition and quantity of intermetallics and carbide phases did not differ. Grain sizes after HT were practically the same (see Table 2, positions 2, 3 and 4 and 5). Difference between metal open and vacuum melting was found in the analysis of phosphorus (decreases by 2 times), sulfur (decreases by 1.5 times), and gases. According to the gas analysis, specimens after vacuum arc remelting contained less (2 times) amount of gases than after open melting, mainly due to hydrogen (3–8 times) and oxygen (2 times) content. Thus, the high content of sulfur, phosphorus, hydrogen, and oxygen affects the characteristics of the nickel alloy 05Cr19Ni55 in air and hydrogen and increases the hydrogen embrittlement.

The relationship between mechanical properties of the alloy and texture that appeared as a result of rolling was investigated. In air, the value of the characteristics of plasticity (δ, ψ) of cylindrical specimens of the alloy (TO1) oriented in the transverse direction (orientation TV) is significantly lower than that of the specimens oriented in the longitudinal direction (LT) (see Table 2, positions 1 and 2). Transversely oriented specimens are more sensitive to hydrogen than longitudinal: δ decreases in 4 and 3.1 times, ψ decreasesin 2.7 and 2.25 times.

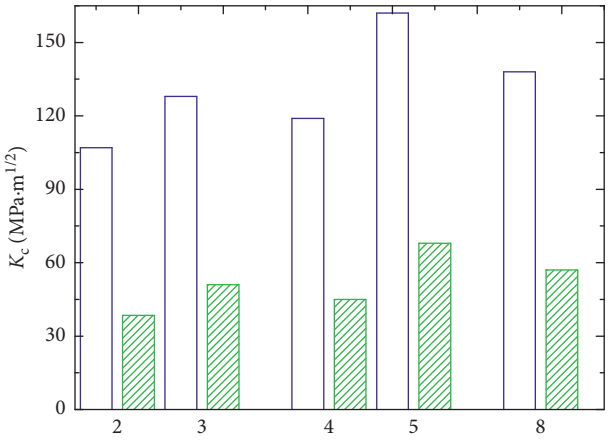

Figure 5: Fracture toughness of specimens of the 05Cr19Ni55 alloy of 20 mm thickness after open and vacuum arc melting in air (light bars) and in hydrogen under pressure 30 MPa after hydrogenation (shaded bars). The numbers near curves correspond to ordinal numbers in Table 2.

Resistance to fracture of the alloy also depends on the orientation of the specimens.

The value of static fracture toughness of compact specimens of 20 mm thickness with cracks oriented in the transverse orientation in air was $K_c = 69$ MPa·m$^{1/2}$ and $K_{Ic}(J) = 86$ MPa·m$^{1/2}$, respectively, which is approximately 20% smaller than that of specimens with cracks oriented in the longitudinal orientation (see Table 2, positions 1 and 2).

In hydrogen, characteristics of crack resistance transversely and longitudinal oriented specimens are 28 and 38.5 MPa·m$^{1/2}$. Similar results were obtained in the study of hydrogen embrittlement of steels 4130 and 4310 and other materials [22–24].

The most likely reason for anisotropy of mechanical properties can be anisotropic structural boundaries in the alloy, i.e., the dependence of fate crack length, falling on the structural boundary, and on the orientation of the applied load. The accumulation of hydrogen at the grain boundaries makes it easy to crack, while at transverse-loading large areas such boundaries are under the influence of normal stresses [21].

The difference in the degree of hydrogen embrittlement of the TV and LT samples is also due, probably, to the formed rolling process by the dislocation texture, which is decisive in hydrogen cracking [12, 13]. In addition, it is known that the effective rate of hydrogen diffusion depends substantially on the orientation of the samples [23].

3.4. Influence of Heat Treatment Regimes and Chemical Composition on the Alloy Properties. Effect of dispersion structure of the alloy on strength, plasticity, and fracture toughness in air and hydrogen was studied. Quenching temperatures were 1253 K, 1283 K, 1323 K, and 1473 K, grain sizes is equal to 21, 36, 85, and 130 microns, respectively, and the average thickness of grain boundaries is 1, 2, 3, and 4 microns (see Figure 6).

After quench from 1473 K alloy has a large grain (Figure 4(c)), small amount of hardening phases, high relative elongation and low strength (Table 2, position 9).

The method of J-integral does not recommend to evaluate the materials static crack resistance in plane-strain conditions. In the absence of large local stresses during the short-term strength tests, arise the minimal embrittlement effect of hydrogen.

For the same aging regimes with decreasing grain size, parameters of plasticity and static crack resistance increased in air and hydrogen (see Table 2, Figure 2, positions 3, 5, 8). At the same time, strength characteristics differ insignificantly. The best combination of mechanical properties in air and greatest resistance to hydrogen embrittlement was observed on longitudinal samples after VAR and HT II (see Table 2, position 4, 5). In this case, the fine-grained structure with equally distributed over the body of grain particles of γ'-phase is obtained. Additional reduction of carbon, nitrogen (from 0.12 to 0.07 mass %), and total content of chromium, molybdenum, niobium, and iron (see Table 1, CC II) leads to the increasing of alloy hydrogen resistance and fracture toughness in air and hydrogen (Table 3).

Probably, this effect is due to a reduction from 3.1 to 2.0 mass % quantity of carbides and carbonitrides (see Table 3, Figure 7), which promote brittle fracture and hydrogen embrittlement of nickel alloys [1–3, 17–19]. It has been found that at low deformation rates (~1 mm/min) and large hydrogen pressures (~3 MPa), intergranular destruction and destruction along the boundaries of the carbide matrix occur with cracking of carbides (Figures 8(a) and 8(b)). The change in the nature of the fracture from transgranular to intergranular under the action of hydrogen is a characteristic feature of dispersion-hard austenitic steels and alloys due to the concentration at the grain boundaries of carbides, intermetallics, and hydrogen [1, 2, 4, 5, 24–27].

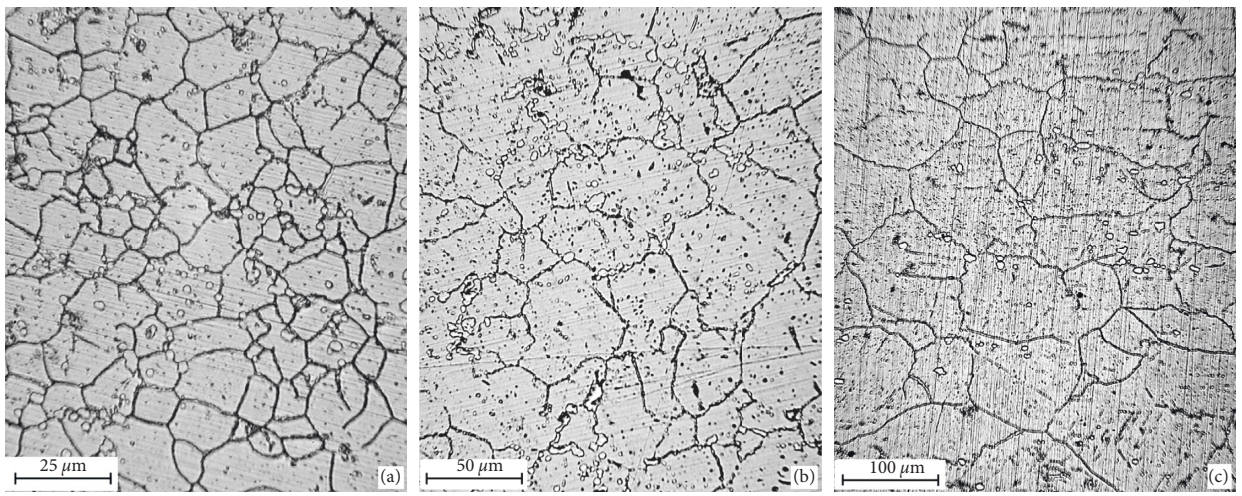

Figure 6: Microstructure of the alloy: after VAR and HT II (a), HT I (b), and HT IV (c).

Table 3: Mechanical properties of alloys with different chemical composition at 293 K and displacement rate 0.1 mm/min.

CC	σ_u (MPa)	σ_{ys} (MPa)	δ %	ψ %	β_ψ	K_c MPa·m$^{1/2}$	$K_{1c}(J_c)$ MPa·m$^{1/2}$	β_{KIc}	(Cr, Ni, Fe)$_{23}$(C, N)$_6$, mass %
I	1080/970	650/660	35/6	38/19	0.50	126/64	162	0.40	3.1
II	1075/1010	630/650	42/12	44/29	0.66	139/89	171	0.52	2.0

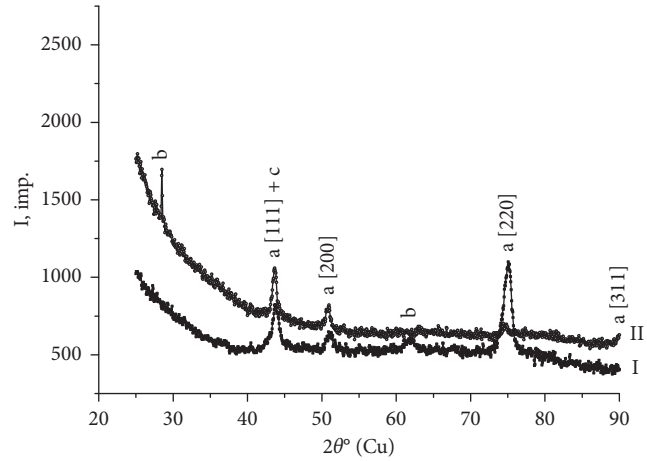

Figure 7: X-ray patterns of the alloys with different content of carbides (I, II, see Table 1): a, Ni-base solid solution; b, Ni_3(Al, Mo, Nb); c, (Cr, Ni, Fe)$_{23}$(C, N)$_6$.

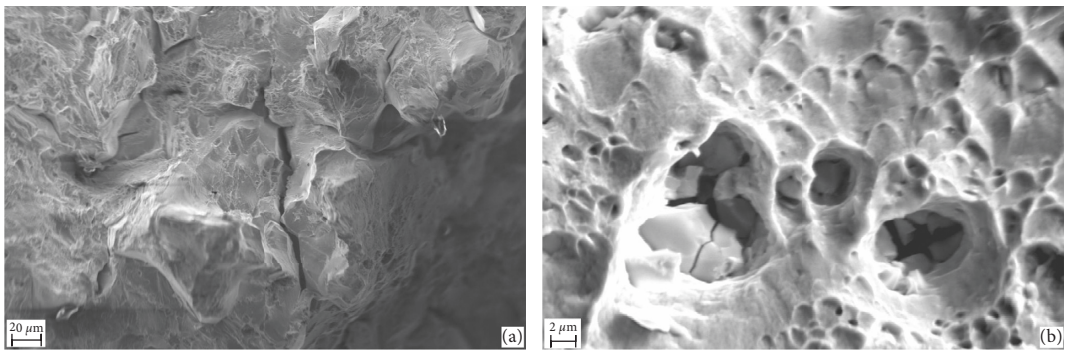

Figure 8: Fracture surface investigation of Ni alloy specimen with cumulation of failure due to static loading at 293 K in hydrogen under the pressure of 30 MPa: (a) intergranular fracture in the area of surface cracks and (b) destruction along the boundary of the carbide matrix with carbide cracking.

4. Conclusions

(1) With the decrease of strain rate from 100 to 0.1 mm/min, plasticity characteristics of the Ni alloy specimens in hydrogen are reduced in the interval rates 0.1–0.01 mm/min. Similarly, the level of K_c decreases with decreasing dK/dt to the minimum value, defined of material structural condition and cumulation of failure.

(2) The values of hydrogen pressure and hydrogen content by which has achieved the maximizing effect on investigated alloys fracture toughness has been established. Compact specimens thickness increasing leads to the hydrogen embrittlement increases. With compact specimen thickness increasing, the hydrogen embrittlement increases.

(3) After cumulation of failure, hydrogen has initiated the fracture by the mechanism of normal separation across the whole crack front, causing formation of the plane-strain state in the specimens.

(4) The alloy properties depend on the orientation of the samples. Strength, plasticity, and fracture toughness in air and hydrogen in transversely oriented specimens are much lower than those in longitudinally oriented specimens.

(5) Vacuum arc remelting, formation of fine structures of the thin grain boundaries, and a minimum number of carbides and carbonitrides have increased fracture toughness and hydrogen resistance of the alloy.

Data Availability

The data used to support the findings of this study are available from the corresponding author upon request.

Conflicts of Interest

The authors declare that they have no conflicts of interest.

References

[1] J. A. Lee, "Hydrogen embrittlement of nickel, cobalt and iron-based superalloys," in *Gaseous Hydrogen Embrittlement of Materials in Energy Technologies Volume 1: The Problem, its Characterisation and Effects on Particular Alloy Classes*, R. P. Gangloff and B. P. Somerday, Eds., pp. 624–667, Woodhead Publishing Limited, Philadelphia. PA, USA, 2012.

[2] M. Dadfarnia, A. Nagao, S. Wang, M. L. Martin, B. P. Somerday, and P. Sofronis, "Recent advances on hydrogen embrittlement of structural materials," *International Journal of Fracture*, vol. 196, no. 1-2, pp. 223–243, 2015.

[3] A. I. Balitskii and V. V. Panasyuk, "Workability assessment of structural steels of power plant units in hydrogen environments," *Strength of Matersials*, vol. 41, no. 1, pp. 52–57, 2009.

[4] R. P. Gangloff, "Science-based prognosis to manage structural alloy performance in hydrogen," in *Effects of Hydrogen on Materials (Proceedings of the 2008 International Hydrogen Conference. Wyoming)*, B. Somerday, P. Sofronis, and J. Russell, Eds., pp. 1–21, ASM International.-Materials Park, Geauga County, OH, USA, 2009.

[5] A. I. Balitskii and L. M. Ivaskevich, "Assessment of hydrogen embrittlement in high-alloy chromium-nickel steels and alloys in hydrogen at high pressures and temperatures," *Strength of Materials*, vol. 50, no. 6, pp. 880–887, 2018.

[6] I. M. Dmytrakh, O. D. Smiyan, A. M. Syrotyuk, and O. L. Bilyy, "Relationship between fatigue crack growth behaviour and local hydrogen concentration near crack tip in pipeline steel," *International Journal of Fatigue*, vol. 50, pp. 26–32, 2013.

[7] J. Lewandowski and D. Rozumek, "Cracks growth in S355 steel under cyclic bending with fillet welded joint," *Theoretical and Applied Fracture Mechanics*, vol. 86, pp. 342–350, 2016.

[8] I. M. Dmytrakh, R. L. Leshchak, A. M. Syrotyuk, and R. A. Barna, "Effect of hydrogen concentration on fatigue crack growth behaviour in pipeline steel," *International Journal of Hydrogen Energy*, vol. 42, no. 9, pp. 6401–6408, 2017.

[9] Z. Zang, G. Obasi, R. Morana, and M. Preuss, "In situ observation of hydrogen induced crack initiation in a nickel-based superalloy," *Scripta Materalia*, vol. 140, pp. 40–44, 2017.

[10] A. I. Balitskii, L. M. Ivaskevich, and V. M. Mochulskyi, "Temperature dependences of age-hardening austenitic steels mechanical properties in gaseous hydrogen," in *Proceedings of the 12th International Conference on Fracture*, M. Elboujdaini, Ed., Ottawa, Canada, July 2009.

[11] A. Balitskii, V. Vytvytskyii, L. Ivaskevich, and J. Eliasz, "The high- and low-cycle fatigue behavior of Ni-contain steels and Ni-alloys in high pressure hydrogen," *International Journal of Fatigue*, vol. 39, pp. 32–37, 2012.

[12] M. A. Mohtadi-Bonab, M. Eskandari, and J. A. Szpunar, "Effect of arisen dislocation density and texture components during cold rolling and annealing treatments on hydrogen induced cracking susceptibility in pipeline steel," *Journal of Materials Research*, vol. 31, no. 21, pp. 3390–3400, 2016.

[13] M. A. Mohtadi-Bonab and H. Ghesmati-Kucheki, "Important factors on the failure of pipeline steels with focus on hydrogen induced cracks and improvement of their resistance: review paper," *Metals and Materials International*, vol. 25, no. 5, pp. 1109–1134, 2019.

[14] A. I. Balitskii, M. Diener, R. Magdowski, V. I. Pokhmurskii, and M. O. Speidel, "Anisotropy of fracture toughness of austenitic high nitrogen chromium-manganese steel," *Materials Science Forum*, vol. 318–320, pp. 401–406, 1999.

[15] A. DI Schino, J. M. Kenny, I. Salvatori, and G. Abbruzzese, "Modelling primary recrystallization and grain growth in a low nickel austenitic stainless steel," *Journal of Materials Science*, vol. 36, no. 3, pp. 593–601, 2001.

[16] A. I. Belogurov, V. S. Rachuk, M. A. Rudis, A. M. Sushkov, and V. I. Kholodnyi, "Strength analysis of structural elements of hydrogen power-generating equipment," *Strength of Matersials*, vol. 40, pp. 814–821, 2004.

[17] A. V. Fishgoit and B. A. Kolachev, "Strength tests in hydrogen in the aerospace industry," *Materials Science*, vol. 33, no. 4, pp. 568–573, 1997.

[18] W. F. Brown and J. E. Srawley, "Plane strain crack toughness testing of high strength metallic materials," vol. 410, ASTM Special Technical Publication, New York, NY, USA, 1966.

[19] *Standard Test Method for JIC, A Measure of Fracture Toughness ASTM STP E 813*, American Society for Testing and Materials, pp. 732–746, Conshohocken, PA, USA.

[20] LECO Corporation, *LECO TCH 600 –Series (Nitrogen, Oxygen, Hydrogen Determination)*, LECO Corporation, St. Joseph, MI, USA, 2003.

[21] A. I. Balitskii, L. M. Ivaskevich, and V. M. Mochulskyi, "Mechanical properties of martensitic steels in gaseous hydrogen," *Strength of Materials*, vol. 44, pp. 64–71, 2012.

[22] A. I. Balitskii, L. M. Ivaskevich, and V. M. Mochulskyi, "Crack resistance of age-hardening Fe-Ni alloys in gaseous hydrogen," in *Proceedings on CD ROM of the 18th European Conference on Fracture. Fracture of Materials and Structures from Micro to Macro Scale*, Dresden, Germany, September 2010.

[23] X. S. Du, W. B. Cao, C. D. Wang, S. J. Li, J. Y. Zhao, and Y. F. Sun, "Effect of microstructures and inclusions on hydrogen-induced cracking and blistering of A537 steel," *Materials Science and Engineering: A*, vol. 642, pp. 181–186, 2015.

[24] A. W. Thompson and I. M. Bernstein, "The role of metallurgical variable in hydrogen-assisted environmental fracture," in *Advances in Corrosion Science and Technology*, M. G. Fontana and R. W. Staehle, Eds., pp. 47–148, Plenum, New York, NY, USA, 1980.

[25] O. I. Balyts'kyi, V. M. Mochylski, and L. M. Ivaskevich, "Evaluation of the influence of hydrogen on mechanical characteristics of complexly alloyed nickel alloys," *Materials Science*, vol. 51, no. 4, pp. 538–547, 2016.

[26] A. I. Balitskii, Y. H. Kvasnitska, L. M. Ivaskevich, and H. P. Mialnitsa, "Hydrogen and corrosion resistance of Ni-Co superalloys for gas turbine engines blades," *Archives of Materials Science and Engineering*, vol. 91, no. 1, pp. 5–10, 2018.

[27] A. Balitskii, V. Mochulskyi, L. Ivaskevich, J. Eliasz, and O. Skolozdra, "Influence of high pressure and high temperature hydrogen on fracture toughness of Ni-containing steels and alloys," *Archive of Mechanical Engineering*, vol. 61, no. 1, pp. 129–138, 2014.